



2 Transfer of satellite rainfall error from gaged to ungaged locations: 3 How realistic will it be for the Global Precipitation Mission?

4 Ling Tang¹ and Faisal Hossain¹

5 Received 27 February 2009; revised 7 April 2009; accepted 29 April 2009; published XX Month 2009.

7 [1] In this study, we investigate the fundamental open
8 question facing the satellite rainfall data community today -
9 If “error” is defined on the basis of independent ground
10 validation (GV) rainfall data, how are these error metrics
11 estimated for a satellite rainfall data product without the
12 need for much extensive GV data? Using a six-year database
13 of high resolution (0.25 degree and 3 hourly) satellite rainfall
14 data over the United States and an optimal spatial
15 interpolation method (ordinary kriging), we demonstrate
16 that certain error metrics (such as bias and probability of
17 detection) are more amenable for ‘transfer’ from gaged to
18 ungaged locations than others. Our findings also indicate that
19 a continuously-calibrated and regionalized error transfer
20 scheme is technically feasible within the neighborhood of a
21 gaged region if more research is carried out on the role played
22 by different interpolation methods and the temporal structure
23 of error. **Citation:** Tang, L., and F. Hossain (2009), Transfer of
24 satellite rainfall error from gaged to ungaged locations: How
25 realistic will it be for the Global Precipitation Mission?, *Geophys.*
26 *Res. Lett.*, 36, LXXXXX, doi:10.1029/2009GL037965.

28 1. Introduction

29 [2] NASA’s planned Global Precipitation Measurement
30 (GPM) mission, in collaboration with other international
31 space partners, will represent a unique constellation of rain
32 measuring satellites comprising passive microwave (PMW)
33 sensors, augmented by a Tropical Rainfall Measuring
34 Mission (TRMM)-like dual-frequency precipitation radar
35 (DPR) [Hou et al., 2008]. GPM is currently scheduled for
36 launch in 2013 (source: gpm.gsfc.nasa.gov) and it will
37 provide high resolution global precipitation products (i.e.,
38 snow and rainfall) with temporal sampling rates ranging from
39 three to six hours and spatial resolution of 25–100 km².
40 Hence, among the various uses, hydrologic application over
41 land will comprise a major avenue through which GPM will
42 be able to demonstrate tangible benefits to society. In
43 particular, the global nature of coherent and more accurate
44 satellite precipitation products (from PMW sensors [see Turk
45 and Miller, 2005]) anticipated from GPM should offer
46 hydrologists tremendous opportunities to improve water
47 resources monitoring in large river basins where rainfall
48 (hereafter used synonymously with ‘precipitation’) is
49 abundant but in situ measurement networks are generally
50 inadequate or declining [Shiklomanov et al., 2002].

51 [3] While the benefits from GPM are conceptually
52 apparent, hydrologists and other users, to varying degrees,

need to know the errors of the satellite rainfall data sets 53
across the range of time/space scales over the whole domain 54
of the data set prior to real-world applications [Hossain and 55
Huffman, 2008]. Representing the error structure of satellite 56
rainfall against quality-controlled ground validation (GV) 57
precipitation datasets is therefore a critical research problem. 58
Recent work has shown that the error structure of satellite 59
precipitation estimates is increasingly complex at smaller 60
scales at which data is now becoming more available 61

[4] Hence, the error of satellite rainfall data represents a 62
paradox that has remained unresolved until today. Satellite 63
rainfall error estimation requires GV rainfall data. On the 64
other hand, satellite data will be most useful over the vast 65
ungaged regions that are lacking in GV data. Depending on 66
how we define GV data, there can be several types of GV 67
‘voids’ where error information will be difficult to be 68
estimated. For example, if we rely on the ‘conventional’ 69
ground source for GV data, voids will be represented by 70
large regions having little or no instrumentation. On the 71
other hand, if a ‘proxy’ for GV is defined, such as the 72
TRMM PR or the proposed GPM DPR, then voids will be 73
numerous grid boxes changing in location with the time- 74
varying satellite overpasses. We are therefore faced with 75
the following unanswered question for GPM- if “error” is 76
defined on the basis of GV data, then how are these error 77
metrics estimated for a global data product without the need 78
for extensive GV data? 79

[5] A middle ground to resolve the above paradox could 80
be to extract error information from a sensor of the highest 81
accuracy currently in orbit (such as the TRMM-like PR on 82
board the GPM) or from nearby sparsely-gaged regions and 83
devise calibrated statistical methods for ‘transfer’ of this 84
error information to the neighboring ungaged regions (see 85
Figure 1 for a conceptual rendition). However, the ‘transfer’ 86
of error information from gaged to ungaged location is 87
clearly an untested idea that needs to be assessed if the 88
benefit of GPM is to be maximized. In this study, our goal is 89
to identify the level to which error can be ‘transferred’ from 90
a gaged (GV) location to a nearby ungaged (non-GV) 91
location. If the idea is found realistic, then the work already 92
accomplished on global classification of precipitation sys- 93
tems [Petersen and Rutledge, 2002] will consequently hold 94
promise for development of a real-time and regionalized 95
error metric scheme for GPM products and their users. 96

2. Study Region, Data, and Spatial Interpolation 98 Method 99

[6] The study region for testing our idea of error ‘transfer’ 100
was the Central United States (US). The geolocation of the 101
four corners of this region are provided in Table 1. Hereafter, 102

¹Department of Civil and Environmental Engineering, Tennessee
Technological University, Cookeville, Tennessee, USA.

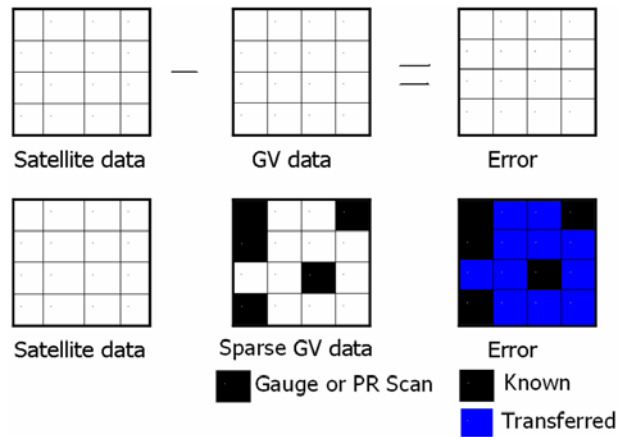


Figure 1. Conceptual rendition of the idea of ‘transfer’ of error information from a gaged (GV) location to an ungaged (non-GV) location. (top) Notion of ‘error’ of satellite rainfall data (in this case, the scalar deviation of magnitudes is termed ‘error’ although there are many other types of error). (bottom) How the known error (derived from GV sites shown (middle) in black) would be ‘transferred’ to the non-GV (ungaged) sites shown (right) in blue.

103 the word ‘transfer’ will be frequently interchanged with
 104 ‘spatial interpolation’. In order to minimize the error of the
 105 GV data in our investigation, we used the National Center
 106 for Environmental Prediction’s (NCEP) 4 km Stage IV
 107 NEXRAD rainfall data that is adjusted to gages over the
 108 US [Fulton *et al.*, 1998; Y. Lin and K. Mitchell, The
 109 NCEP Stage II/IV hourly precipitation analyses: Develop-
 110 ment and applications, paper presented at the 19th AMS
 111 Conference on Hydrology, American Meteorological
 112 Society, San Diego, California, 2005]. NASA’s near real-
 113 time satellite rainfall data-products from PMW calibrated
 114 Infrared (IR) and merged PMW-IR estimates and labeled
 115 as 3B41RT and 3B42RT, respectively, were used as the
 116 satellite rainfall data [Huffman *et al.*, 2007]. These are
 117 globally available on a near real-time basis at 0.25 degree and
 118 1–3 hourly resolution from the world wide web (see ftp://
 119 trmmopen.gsfc.nasa.gov). The data for GV and satellite
 120 rainfall data spanned the period of 2002–2007 (6 years). A
 121 point to note is that there also exists research-grade satellite
 122 product 3B42 (V6) that is produced by NASA retrospectively
 123 by adjusting the bias using gage rainfall. Although the
 124 research grade product of 3B42 (V6) is known to have lower
 125 levels of uncertainty, this study focused on the testing the
 126 concept of transfer in the operational mode using real-time
 127 (RT) products.

128 [7] The method of ordinary kriging (OK) was used for
 129 testing the ‘transfer’ of error metrics from a gaged to an
 130 ungaged location. Ordinary kriging is the most common
 131 spatial interpolation estimator $\hat{Z}(x_0)$ used to find the best
 132 linear unbiased estimate of a second-order stationary random
 133 field with an unknown constant mean as follows:

$$\hat{Z}(x_0) = \sum_{i=1}^n \lambda_i Z(x_i) \quad (1)$$

where $\hat{Z}(x_0)$ = kriging estimate at location x_0 ; $Z(x_i)$ = sampled
 value at location x_i ; and λ_i = weighting factor for $Z(x_i)$. For
 further details on the method of OK, the reader is referred
 to Deutsch and Journel [1992].

3. Methodology

[8] The NEXRAD Stage IV GV rainfall data was first
 remapped to 0.25 degree 3 hourly resolution for consistency
 with the native scale of the satellite rainfall products. Four
 widely-used error metrics were then computed for 3B41RT
 and 3B42RT products over the 6 year period to derive a
 relatively stationary spatial field of ‘climatologic’ error
 metrics for the study region. These metrics were: Bias
 (BIAS), Root Mean Squared Error (RMSE), Probability of
 Detection (POD) and False Alarm Ratio (FAR). The reader
 is referred to Ebert *et al.* [2007] for the formulation of these
 error metrics.

[9] Spatial correlograms for each error metric were
 derived and the correlation length (CL), where the auto-
 correlation dropped to 1/e (e-folding distance), was then
 computed. Next, the empirical semi-variograms were derived
 and then idealized as exponential semi-variogram functions
 prior to the kriging interpolation as follows,

$$\gamma(h) = c_0 + c(1 - e^{-h/a}) \quad (2)$$

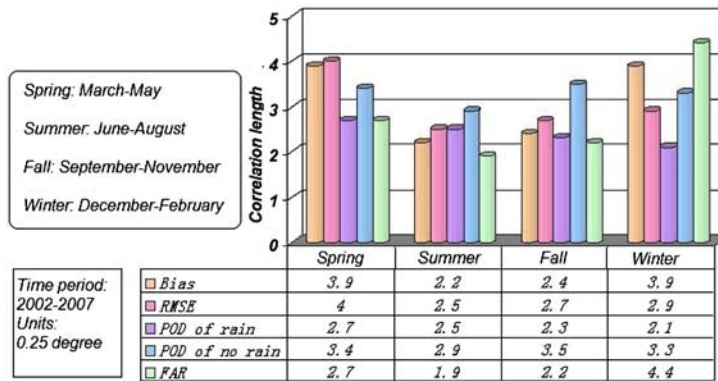
where $\gamma(h)$ is the semi-variance at spatial lag ‘h’, c_0
 represents the nugget variance (i.e., the minimum variability
 observed or the ‘noise’ level at the smallest separating
 distance equals 0; c is the sill variance – when spatial lag is
 infinite; and a is the correlation length. Figure 2 provides a
 summary of the ‘climatologic’ correlation length (e-folding
 distance) by season for various error metrics of the satellite
 rainfall products.

[10] Assuming that only 50% of the region was gaged
 (having access to GV data), kriging was implemented to
 estimate error metrics at the other 50% of the ungaged
 region (lacking in GV data; see Figure 1). This is analogous
 to a data withholding exercise using the dependent data.
 Selection of gaged grid boxes was random and hence each
 kriging realization was repeated 10 times in a Monte Carlo
 (MC) fashion to derive an average scenario of the ensemble.
 The semi-variogram and correlation length were computed
 on the basis of the 50% of the assumed ‘available’ data. To
 keep the matrix computations of kriging efficient, spatial
 interpolation was performed using a smaller square-sized
 ‘window’ around the ungaged grid box in place of the entire
 collection of gaged grid boxes in the whole region. The
 sides of this square window were equal to the correlation
 length of the error metric being ‘transferred’. Preliminary

Table 1. Geolocation of the Four Corners of the Study Region
 Shown in Figure 3

	Longitude (West)	Latitude (North)	
Upper left corner	–104.5	43.5	t1.3
Upper right corner	–88.25	43.5	t1.4
Lower left corner	–104.5	33.5	t1.5
Lower right corner	–88.5	33.5	t1.6

**3B41RT Analysis on Spatial Structure per Season
(Correlation Length)**



**3B42RT Analysis on Spatial Structure per Season
(Correlation Length)**

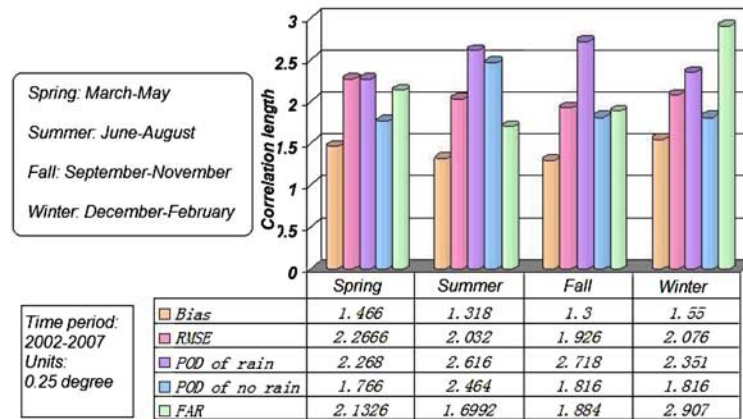


Figure 2. Correlation length of error metrics for (top) 3B41RT and (bottom) 3B42RT shown as a function of season. Note the distance unit is 0.25 degree grid boxes (~25 km). The vertical bars are shown in order from left to right as ‘Bias’, ‘RMSE’, ‘POD rain’, ‘POD no-rain’, ‘FAR’.

182 analyses showed that such a moving window based kriging
 183 was justified as the interpolation weights λ_i (equation (1))
 184 due to grid boxes farther than one correlation length were
 185 found to be zero.

186 **4. Results**

187 [11] Figure 3 shows the performance of kriging at
 188 non-GV grid boxes for the BIAS of 3B41RT. It appears
 189 that the transfer of bias via kriging does not lead to whole-
 190 sale changes in the pattern of the error field when compared
 191 to the true climatologic error field (see Figure 3, left).
 192 However, a more rigorous assessment can be obtained
 193 through the comparison of the histograms (probability distri-
 194 bution) of kriging error with the marginal distribution of
 195 the kriging estimate. Herein, the kriging error is defined as the
 196 scalar difference between the kriged error metric and the true
 197 error metric. If indeed the transfer or error metric is robust
 198 then the kriging error distribution should have a near-zero
 199 mean (for unbiasedness) and a lower spread (minimum error
 200 variance) compared to the marginal distribution of the

201 estimated error. Figures 4 and 5 show the comparison of the
 202 histograms for 3B41RT and 3B41RT for BIAS and POD,
 203 respectively. It is seen that for BIAS, the error histogram due
 204 to kriging has smaller variance compared to the marginal
 205 histogram of kriging estimates. Table 2 summarizes the
 206 correlation between kriging estimated error and true value
 207 of error for different error metrics.

208 [12] As a preliminary analysis, the use of an optimal spatial
 209 interpolation method, such as ordinary kriging, for the
 210 transfer of error metrics appears promising at ungaged
 211 locations. Of the four error metrics studied, Bias, followed
 212 by POD, was found to be most amenable for transfer. Across
 213 satellite data products, kriging appears more effective for
 214 the IR-based 3B41RT than the multi-sensor PMW-IR-based
 215 3B42RT. This is not unexpected because of the lower
 216 correlation length and spatial dependency of error metrics
 217 for 3B4R2T. The grid boxes pertaining to non-PMW over-
 218 passes for the 3B42Rt product are essentially supplied from
 219 the 3B41RT product. This simple style of mosaicing a dataset
 220 from two different spatial random fields, while improving the
 221 quality of rainfall estimate in terms of bias and RMSE,

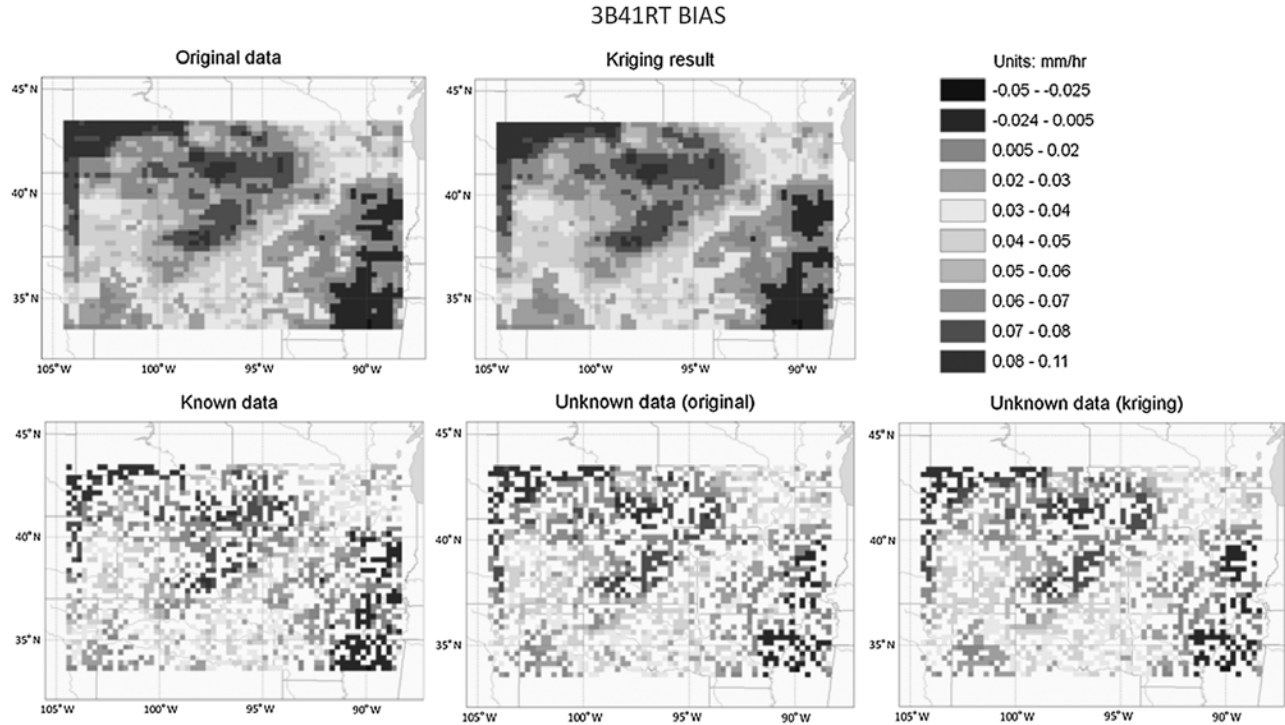


Figure 3. Transfer of BIAS of 3B41RT from gaged to ungaged locations. (top left) True field of error on bias based on 6 years of data. (bottom left) The randomly selected 50% of the region for computation of the empirical variogram and correlation length. (bottom middle) The other 50% of the region that is assumed to be non-GV grid boxes. (bottom right) The estimation of the bias at the non-GV grid boxes using kriging.

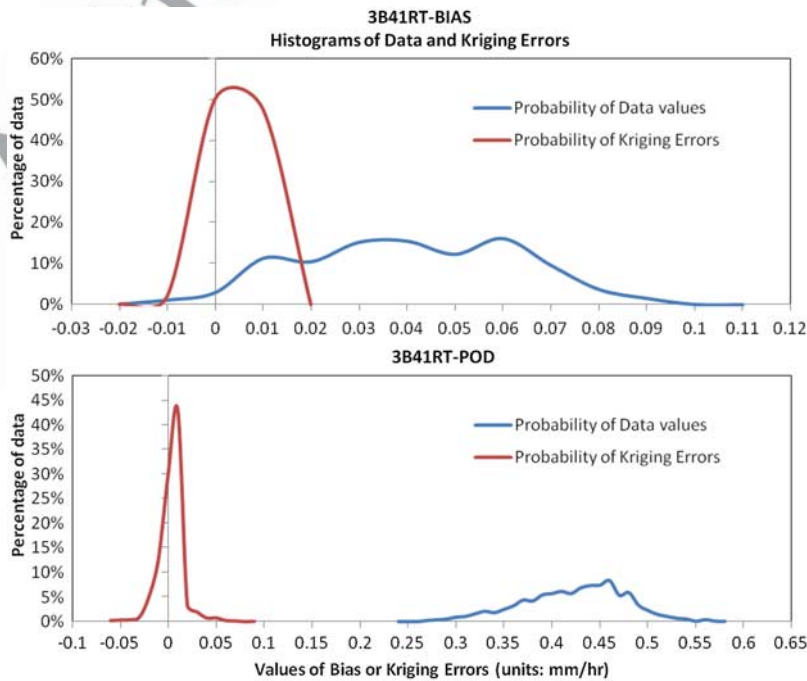


Figure 4. Comparison of histograms of kriging errors and kriging values for 3B41RT (top) BIAS and (bottom) POD.

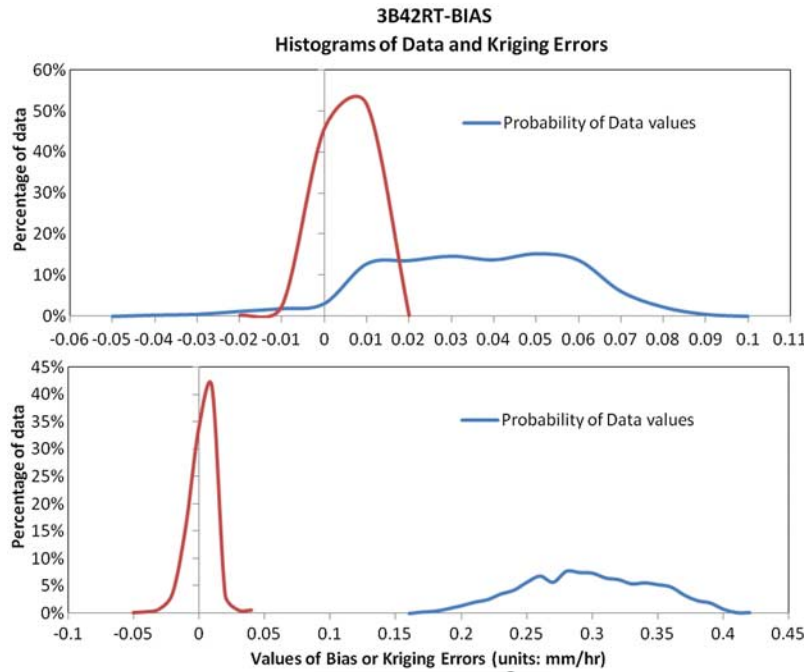


Figure 5. Comparison of histograms of kriging errors and kriging values for 3B42RT (top) BIAS and (bottom) POD.

222 actually lowers the spatial structure by adding more spatial
 223 randomness to the data.

224 **5. Discussion**

225 [13] Overall, our assessment indicates that it is indeed
 226 technically possible to transfer error metrics from a gaged to
 227 an ungaged location for certain error metrics and that a
 228 regionalized error metric scheme for GPM may one day be
 229 possible. However, our work has also opened a much wider
 230 range of issues that require research before such a system
 231 can be implemented for GPM. First, the choice of randomly
 232 selected 50% of grid boxes may be somewhat unrealistic
 233 during the GPM era. Such a randomly selected combination
 234 of grid boxes is perhaps realistic if the use of the orbiting
 235 GPM PR is considered as the only source for GV data for
 236 the transfer of error metrics. The role played by the fraction
 237 of a region missing in GV data on the effectiveness of
 238 transfer or error also needs to be investigated. Another aspect
 239 that needs to be studied is the assumption of stationarity of
 240 error metrics that is critical for kriging. If a system is desired
 241 that can routinely provide an estimate of time-varying error
 242 metrics at ungaged locations in lieu of ‘climatologic’ values
 243 for a region, then the temporal structure of errors would need
 244 to be analyzed first.

[14] **Acknowledgments.** The first author (Tang) was supported by the 245
 NASA Earth System Science Fellowship (2008–2011). The second author 246
 (Hossain) was supported by the NASA New Investigator Program Award 247
 (NNX08AR32G). 248

References

Deutsch, C., and A. Journel (1992), *GSLIB: Geostatistical Software Library* 250
and User’s Guide, 340 pp., Oxford Univ. Press, Oxford, U. K. 251
 Ebert, E. E. (2008), Fuzzy verification of high resolution gridded forecasts: 252
 A review and proposed framework, *Meteorol. Appl.*, 15, 51–64. 253
 Ebert, E. E., J. E. Jonowiak, and C. Kidd (2007), Comparison of near real- 254
 time precipitation estimates from satellite observations and numerical 255
 models, *Bull. Am. Meteorol. Soc.*, 88, 47–64. 256
 Fulton, R. A., J. P. Breidenbach, D.-J. Seo, D. A. Miller, and T. O’Bannon 257
 (1998), The WSR-88D rainfall algorithm, *Weather Forecast.*, 13, 258
 377–395. 259
 Hossain, F., and G. J. Huffman (2008), Investigating error metrics for 260
 satellite rainfall at hydrologically relevant scales, *J. Hydrometeorol.*, 9, 261
 563–575. 262
 Hou, A., G. S. Jackson, C. Kummerow, and C. M. Shepherd (2008), Global 263
 precipitation measurement, in *Precipitation: Advances in Measurement,* 264
Estimation, and Prediction, edited by S. Michaelides, pp. 1–39, Springer, 265
 Berlin. 266
 Huffman, G. J., R. F. Adler, D. T. Bolvin, G. Gu, E. J. Nelkin, K. P. 267
 Bowman, Y. Hong, E. F. Stocker, and D. B. Wolff (2007), The TRMM 268
 multi-satellite precipitation analysis: Quasi-global, multi-year, combined 269
 sensor precipitation estimates at fine scales, *J. Hydrometeorol.*, 8, 28–55. 270
 Petersen, W. A., and S. A. Rutledge (2002), Regional variability in tropical 271
 convection: Observations from TRMM, *J. Clim.*, 14, 3566–3586. 272
 Shiklomanov, A. I., R. B. Lammers, and C. J. Vörösmarty (2002), Wide- 273
 spread decline in hydrological monitoring threatens pan-arctic research, 274
Eos Trans. AGU, 83(2), 16–17. 275
 Turk, F. J., and S. D. Miller (2005), Toward improving estimates of remotely- 276
 sensed precipitation with MODIS/AMSR-E blended data techniques, 277
IEEE Trans. Geosci. Remote Sens., 43, 1059–1069. 278

t2.1 **Table 2.** Correlation Between Kriged Estimate of an Error Metric
 and the True Climatologic Value

t2.2 Error Metrics	Bias	RMSE	POD	FAR
t2.3 3B41RT	0.5752	0.1647	0.5076	0.2004
t2.4 3B42RT	0.4864	0.1465	0.5134	0.2902

F. Hossain and L. Tang, Department of Civil and Environmental 280
 Engineering, Tennessee Technological University, 1020 Stadium Drive, 281
 Cookeville, TN 38505-0001, USA. (fhossain@tntech.edu) 282